CHEMISTRY
A EUROPEAN JOURNAL

DOI: 10.1002/chem.201102961

Synthesis and Characterization of Photoswitchable Fluorescent SiO_2 Nanoparticles

Florian May,[a] Michael Peter,[a] Andreas Hütten,[b] Luca Prodi,[c] and Jochen Mattay*[a]

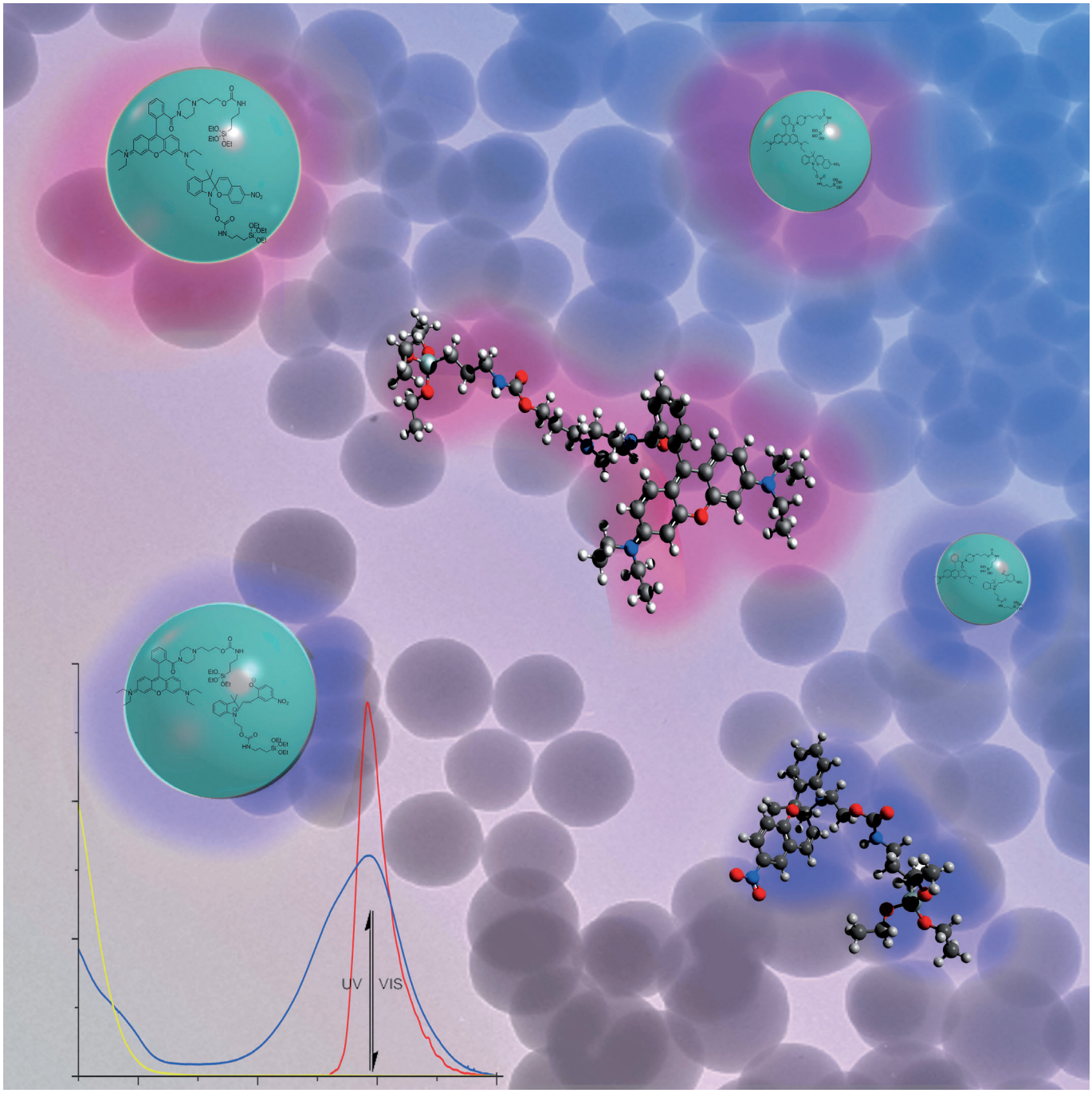

Abstract: Switchable fluorescent silica nanoparticles have been prepared by covalently incorporating a fluorophore and a photochromic compound inside the particle core. The fluorescence can be switched reversibly between an on- and off-state via energy transfer. The particles were synthesized using different amounts of the photoswitchable compound (spiropyran) and the fluorophore (rhodamine B) in a size distribution between 98 and 140 nm and were characterized in terms of size, switching properties, and fluorescence efficiency by TEM, and UV\Vis and fluorescence spectroscopy.

Keywords: fluorescence spectroscopy · FRET · rhodamine · silica nanoparticles · spiropyran

Introduction

Optical fluorescence microscopes use visible light to provide us with magnified images of small samples and play a key role, for example, for in vivo imaging in life sciences. However, their resolution is limited to approximately 200 nm in the focal plane and therefore prohibits the examination of much smaller cellular objects.[1] New methods of so called subdiffractional optical fluorescence microscopy were developed that provide enhanced optical resolution in the range of 20–100 nm.[2–5] Some of these methods depend on modulating the fluorophore's emission between a dark off- and a bright on-state.

Photochromic compounds such as spiropyrans can be reversibly switched between a non-colored closed-ring state (SP, spiroform) and a colored open state (MC, merocyanine form) by irradiation with light and are therefore often referred to as photoswitches (Figure 1).[6]

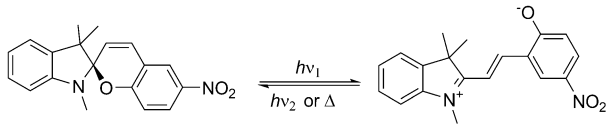

Figure 1. The spiroform (closed) and the merocyanine form (open) of a spiropyran.

These states exhibit different chemical and physical properties,[7] which enables the merocyanine to act as a resonance energy acceptor to quench a fluorophore's emission in a so called Förster resonance energy transfer (FRET) while the spiroform does not influence the fluorophore.[8] Thus, the fluorescence of a fluorophore can be modulated between on and off by switching the spiropyran between the closed and open state (Scheme 1).

The efficiency of the FRET process strongly depends on the matching of the energy levels of the donor fluorophore and the acceptor photoswitch as well as on the distance and orientation of the donor–acceptor pair as shown more than 60 years ago by Förster in his seminal report,[9] and more recently at a quantum electrodynamic level by Andrews and Bradshaw,[10] and for photoswitchable acceptors such as dithienylethenes, for example, by Irie,[11] Branda,[12] Li,[13] and their co-workers.

However, low solubility in aqueous media, relatively fast decomposition, and toxicity limit the applicability of photoswitchable fluorophores in biological systems, especially for spiropyrans.[8,14] Silica nanoparticles (silica NP) may offer a solution to these problems.[15–17] For example, fluorescence dye doped silica NP have already been used in fluorescence microscopy, because they are hydrophilic, biocompatible, and can easily be modified with biomolecules.[18]

Usually, photoswitchable fluorescent NP are non-covalently doped with the fluorophores and photoswitches after formation of the particle, which leads to dye leaking and an interaction of the dye with its surrounding making fluorescence spectroscopy difficult (for NP doped with fluorescence dyes see references [16–22]). For example, Li and co-workers used a perylene as fluorophore and a spiropyran derivative as acceptor in polymeric NP generated by microemulsion polymerization capable of switchable dual-fluorescence.[23] Unfortunately, polymeric NP are subject to pH-dependent swelling and agglomeration and therefore lead to bleeding effects and changing of physical properties in different solvents.[24–26]

On the other hand, silica nanoparticles have significant advantages compared to polymethylmethacrylate (PMMA) or particles obtained from the bulk material by the top–down approach because they are immune to dwelling and easy to modify as shown for those made by the Stöber method from silyl ether as precursor in ammonia solution.[15,24,25] For example, Hell and co-workers covalently incorporated a diarylethene-atto dye conjugate in silica NP and gained a functional FRET based system.[19] Most recently we also reported on reversible photoswitching of dye-doped core-shell silica nanoparticles with a dithienylethene derivative incorporated into the outer shell.[27]

[a] F. May, M. Peter, Prof. Dr. J. Mattay
Organic Chemistry I, Department of Chemistry
Bielefeld University, P. O. Box 100131
35501 Bielefeld (Germany)
Fax: (+49) 521-106-6146
E-mail: mattay@uni-bielefeld.de

[b] Prof. Dr. A. Hütten
Thin Films & Physics of Nanostructures, Department of Physics
Bielefeld University, 35501 Bielefeld (Germany)

[c] Prof. Dr. L. Prodi
Dipartimento di Chimica "G. Ciamician"
Università degli Studi di Bologna
Via Selmi 2, 40126 Bologna (Italy)

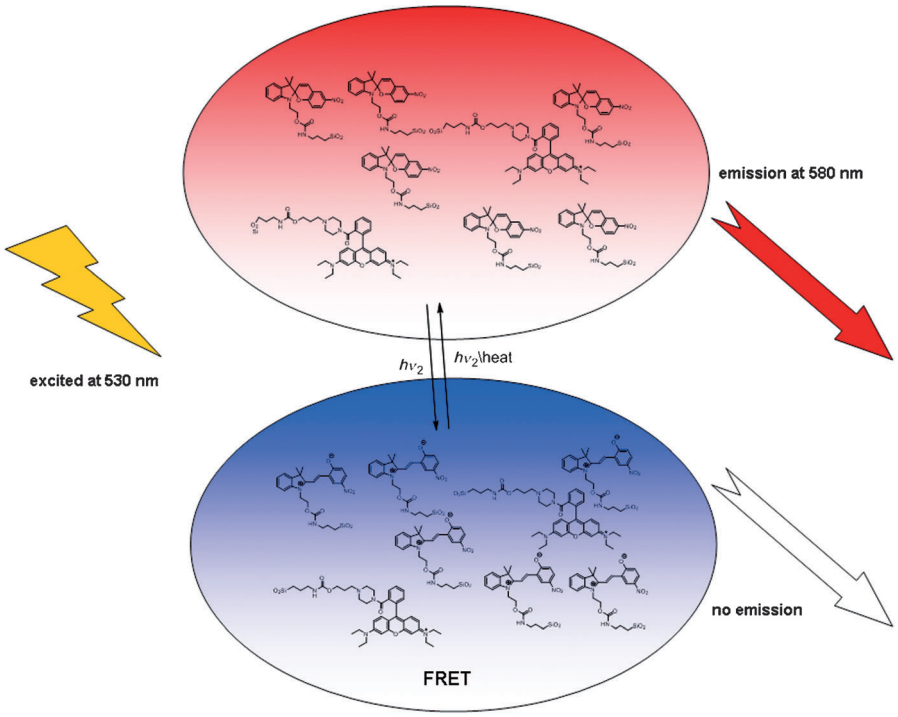

Scheme 1. Principle of fluorescence quenching via a FRET mechanism. The spiropyran (SP) and the rhodamine compound (RH) are both covalently incorporated inside the silica nanoparticle.

Herein we wish to report the synthesis and properties of spiropyran (SP) **1** and a rhodamine B (RH) derivative **2** (Figure 2), their covalent incorporation inside silica NP and

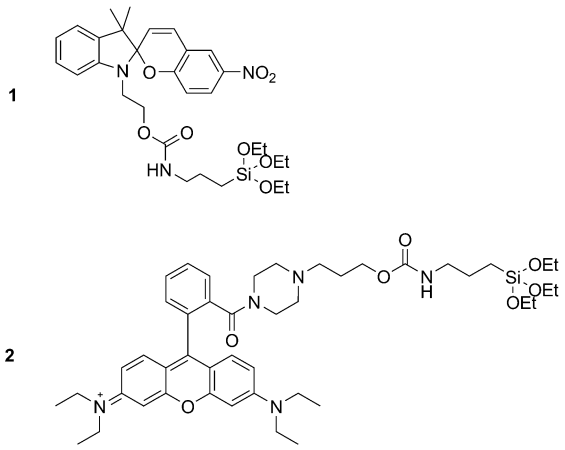

Figure 2. Spiropyran (**1**) and rhodamine B derivative (**2**) used for the nanoparticle synthesis.

their spectroscopic properties regarding photoswitchable fluorescence. We chose spiropyran as photoswitch since its merocyanine form is stabilized through the Si–OH and Si–O groups of the silica which leads to a long living merocyanine form.[28]

Results and Discussion

Assuming a Förster resonance energy transfer (FRET), the emission band of the fluorophore (donor) need to overlap with the absorption band of the photochromic compound in its on-state (acceptor) and the distance between both should be within the Förster radius. Rhodamine B (**2**; donor) and spiropyran (**1**; acceptor) are perfectly suited for the quenching process due to their well matching emission and absorption bands (Figure 3): while **1** does not show any absorption in its spirocyclic form that overlaps with the emission of 2 at 590 nm and therefore does not influence the fluorescence in its closed off-state, the merocyanine obtained after UV irradiation shows a strong overlap and therefore quenches the rhodamine B fluorescence.

In this work we used derivatives of both suitable for covalent linking within the interior of silica NPs. In addition, rhodamine B is cheap, easy to modify, and photochemically stable with good properties for fluorescence spectroscopy (high quantum yield, good stability).

To covalently bind the photoswitch and the fluorophore to the silica matrix of NP, silylester derivatives **1** and **2** were synthesized (Figure 2). The functionalized precursors were given to a solution of ethanol, ammonia, TEOS and water, generally used for NP synthesis.[29] By this procedure we

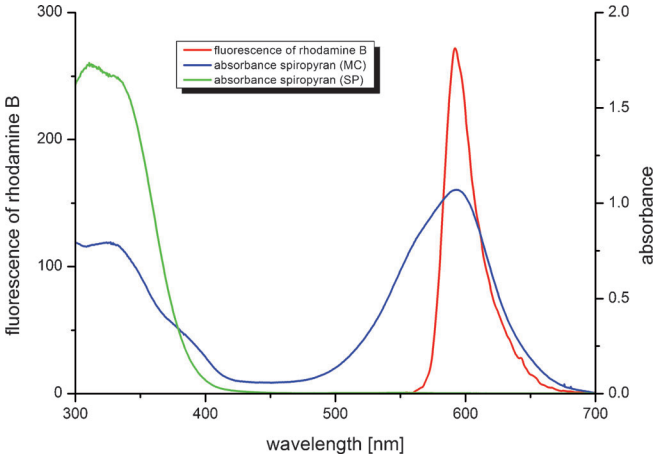

Figure 3. Superposition of the fluorescence maxima of rhodamine B (**2**) (red line) and the absorbance of the spiropyran (**1**) in the open form (MC, blue line) and in the closed form (SP, green line).

were able to establish a stable and photoswitchable fluorescent system, without the usual leaking and swelling effects.

The general method for the synthesis of spiropyrans is the condensation of an indoline derivative with a nitrosalicylaldehyde (Figure 4, see the Experimental Section for details).

Indoline **4** was obtained by alkylation of commercially available 2,3,3-trimethyl-3*H*-indole with 3-bromoethanol and subsequent treatment with potassium hydroxide in 61% yield.[26] Condensation with commercially available 5-nitrosalicylaldehyde **5** gave the photochromic 3′,3′-dimethyl-1′-(β-hydroxyethyl)-6-nitrospyro-[2*H*-1]benzopyran-2,2′-indoline) (**6**) in 82% yield.[30] Finally reaction of **6** with 3-(triethoxysilyl)propylisocyanate (**7**) in dry DMF gave the desired photochromic silylester 1′-(3-triethoxysilanpropyl)-3′-dimethyl-nitrospyro[2*H*-1]benzopyran-2,2′-indoline (**1**) in 69% yield.[29]

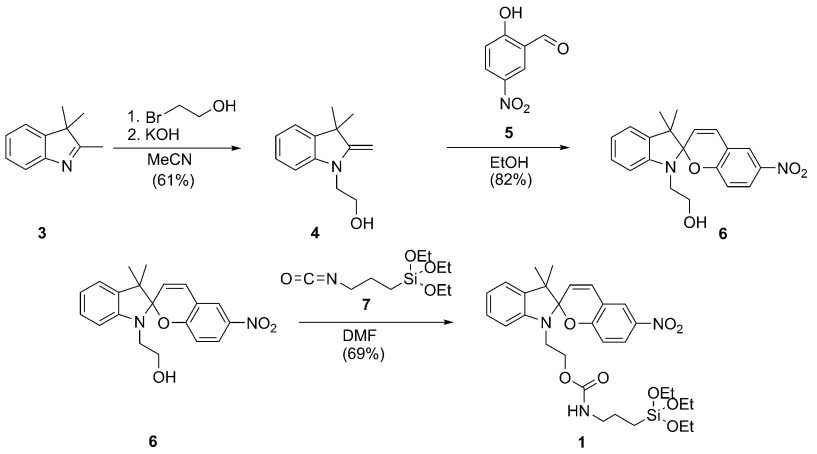

Figure 4. Synthesis of spiropyran-silylester (**1**).[29]

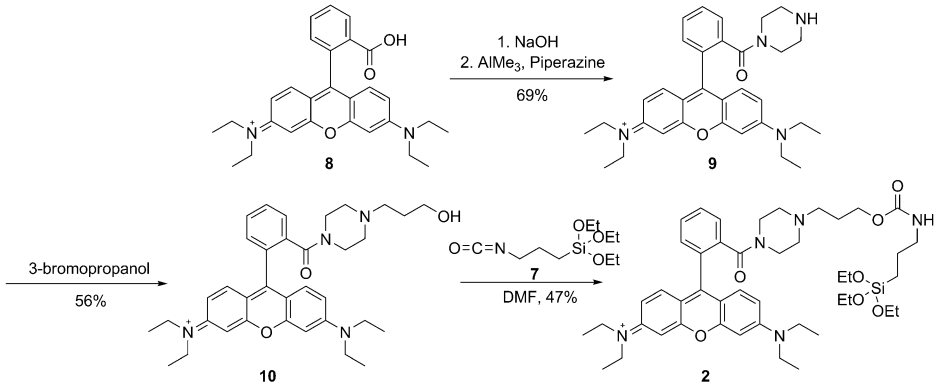

Figure 5. Synthesis of rhodamine B derivative (**2**).[31]

Functionalization of rhodamine B with primary amines via amide formation is known to be limited because of cyclization to the non fluorescent lactame under basic conditions. In order to link rhodamine B to the matrix of silica NP secondary amines are required. Therefore we chose an earlier reported piperazine-approach to prevent the cyclisation to the lactame.[31] The synthesis of the piperazine-linked silylester **2** is depicted in Figure 5.

Commercially available rhodamine B (**8**) was converted to the piperazine-amide **9** in 69% yield as reported in the literature.[31] After alkylation of **9** with 3-bromopropanol to give alcohol **10** in 56% yield the reaction with 3-(triethoxysilyl)propylisocyanate **7** gave the rhodamine B 4-(3-triethoxysilanpropyl)piperazine amide **2** in 47% yield.

The nanoparticles were prepared via the Stöber method from TEOS, ammonia solution in ethanol/water, and stirring at room temperature overnight. Further, we examined different molar ratios of the precursor materials to analyze their effect on the NP morphology.

Different amounts of spiropyran **1** and rhodamine **2** were added to the emulsion of the precursor (Table 1).

After centrifugation and washing with water/ethanol (1:1) we obtained several nanoparticle samples. They differ in

Table 1. Reaction conditions for the preparation of the NPs and their specific properties.

Sample	**1** [mmol]	**2** [mmol]	Method[a]	Diameter [nm][b]	Decline of emiss. intensity [%][c]
NP-1	0.09	0.003	A	112	61
NP-2	0.45	0.0015	A	104	58
NP-3	0.09	0.0003	A	141	63
NP-4	0.18	0.006	A	102	67
NP-5	0.09	0.003	B	113	64
NP-6	0.45	0.015	B	106	67
NP-7	0.09	0.0003	B	125	65
NP-8	0.18	0.006	B	70	68
NP-9	0.09	0.00003	A	100	76
NP-10	0.18	0.00006	A	98	89
NP-11	0.09	–	A	108	–
NP-12	–	0.00009	A	150	–
NP-13	–	–	A	170	–

[a] Two different molar ratios of TEOS/NH_3/EtOH/H_2O were used. A: TEOS (2 mL), ammonia solution (2 mL), double distilled water (6 mL), EtOH (100 mL). B: TEOS (4 mL), ammonia solution (4 mL), double distilled water (12 mL), EtOH (200 mL). [b] Average diameter, calculated from TEM measurements. [c] All emission intensities are normalized and taken at the emission maxima of 593 nm. The decline is given in percent.

size distribution from 70 up to 170 nm, examples are shown in Scheme 2.

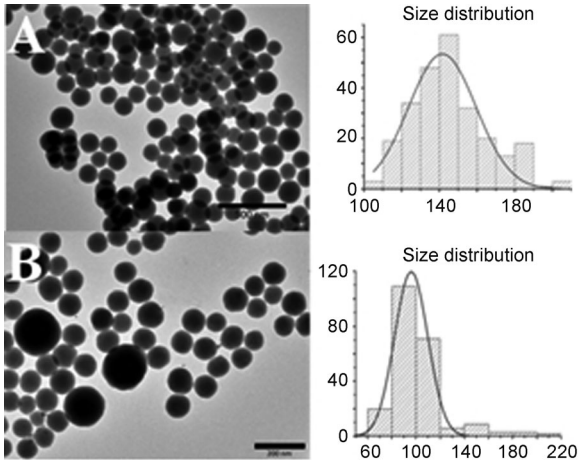

Scheme 2. TEM images and the corresponding size distribution of NP-3 (A) and NP-10 (B).

These nanoparticles are totally suitable for application in confocal and high resolution fluorescence microscopy. Our particles are smaller than the normally used microbeads, which are in the micrometer scale, but smaller ones can be used as well. In the high resolution fluorescence microscopy particles with sizes between 40 and 200 nm are used with great success.[32,33]

The size distribution of the doped NP decreases with higher molar ratios of the photoswitch and the fluorophore in relation to the precursor (Figure 6), which corresponds to the theory of formation of nanoparticles.

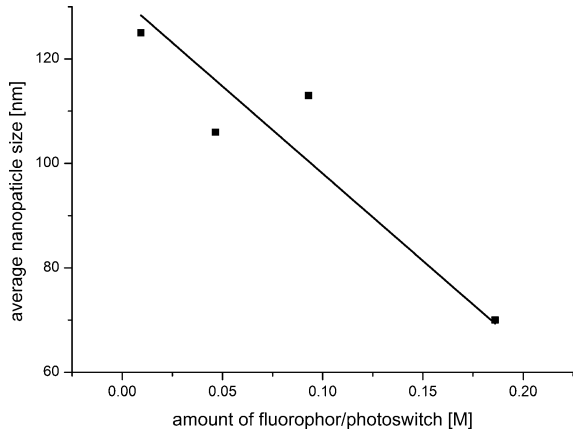

Figure 6. Average size of the nanoparticles plotted against the amount of fluorophore (**2**) and photoswitch (**1**) obtained via method B (Table 1).

For a better understanding of this effect it is necessary to take a closer look at the theory of particle synthesis established by LaMer et al.[34] The synthesis of nanoparticles (NP) starts with the decomposition of the precursor (in this case TEOS) to the monomer, which forms the NP by nucleation. In literature two possible nucleation processes are known, the homogeneous[34] and the heterogeneous one (LaMer model), both are mechanistically similar to the classical crystallization theory. In case of heterogeneous nucleation, the average diameter of the NP shrinks in relation to the concentration of the additive, similar to crystallization seeds. More seeds result in smaller particles because less material can be decomposed on each particle. In case of homogeneous nucleation, the diameter either grows or subsides in relation to the concentration of the precursor, that is, the number of nuclei only depends on the concentration of the monomer (TEOS).[34] The concentration of TEOS was constant during the synthesis, however, we could not observe a constant diameter as we would expect for a homogeneous nucleation process. On the contrary, the decrease in the diameter with increasing amount of **1** and **2** is nearly linear (Figure 6) indicating a heterogeneous nucleation process rather than a homogeneous nucleation of precursor (TEOS) itself.

These doped NP were studied with regard to their fluorescence modulation. Switching from the spiroform to the merocyanine of the spiropyran (**1**) took place at 350 nm, the back reaction proceeds at 590 nm (Figure 7). As expected the merocyanine is thermally stable, no back reaction could be observed after 24 h, in contrast to the spiropyran in ethanolic solution, here the back reaction occurred after 30 min.[35]

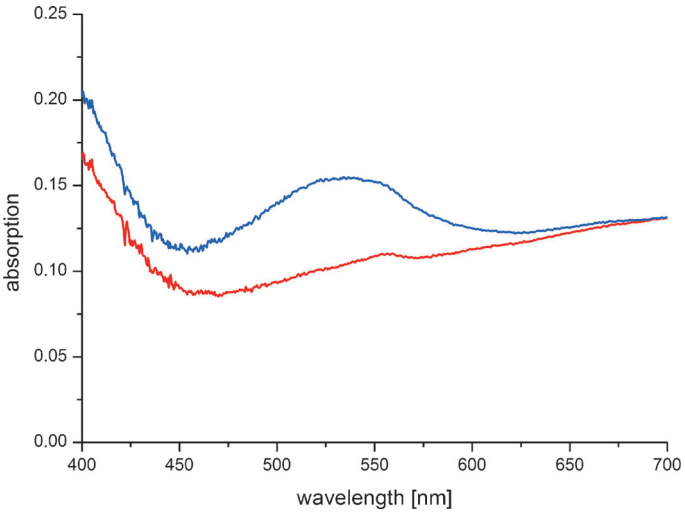

Figure 7. UV/Vis-absorption spectra of NP-10 against a reference of NP-13 (without doping) after irradiation with UV light (350 nm, blue line) and after irradiation with Vis-light (590 nm, red line).

Thus we have synthesized a system with stable properties in the timescale of a typical fluorescence experiment.

NP-10 shows a relative (to rhodamine B) quantum yield of $\theta = 0.15$ in the on-state. The fluorescence emission spectra before and after irradiation with UV light (350 nm) of both NP-8 and NP-10 are shown in Figures 8 and 9.

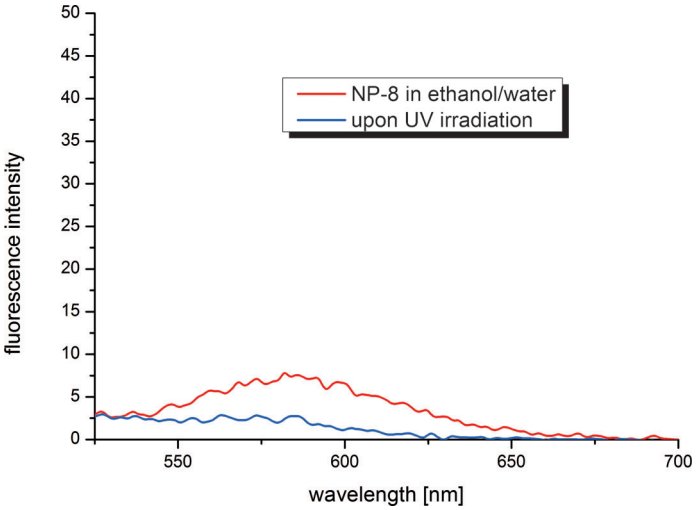

Figure 8. Fluorescence emission spectra of NP-8 (3×10^{-4} mol) in ethanol before (red line) and after (blue line) irradiation with UV light (350 nm, 30 s).

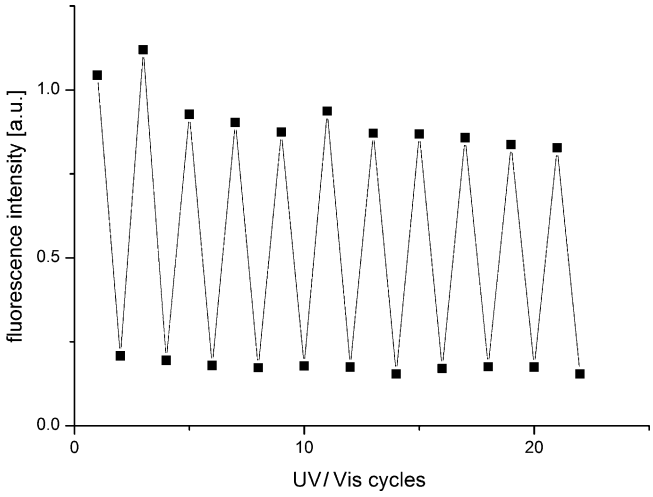

Figure 10. Fluorescence intensity ($\lambda_{ex}=520$ nm) switching cycle of NP-10 (3×10^{-4} M) by irradiation with UV (350 nm, 30 s) and Vis light (590 nm, 60 s), recorded at 593 nm.

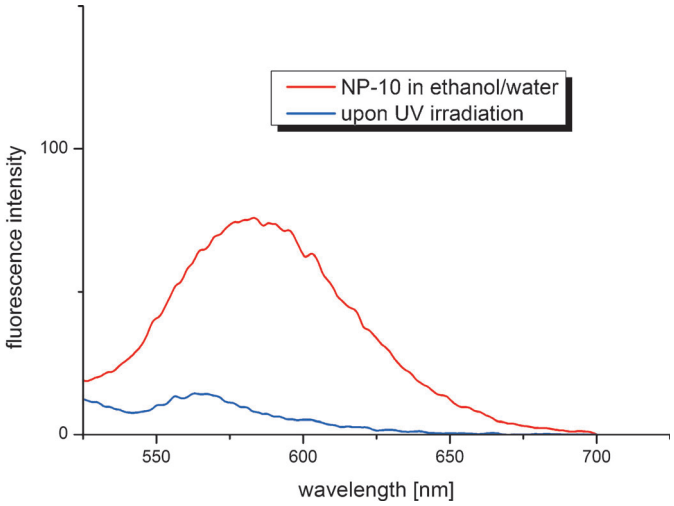

Figure 9. Fluorescence emission spectra of NP-10 (3×10^{-4} M) in ethanol before (red line) and after (blue line) irradiation with UV light (350 nm, 30 s).

For example, the fluorescence of NP-10 vanishes almost quantitatively (see Table 1) upon irradiation at 350 nm. We assume that the hypsochromic shift in the remaining fluorescence is caused by the fluorescence of the spiropyran in its merocyanine form.[36–39] However, with a quantum yield of $\theta=0.006$ (relative to rhodamine B) this luminescence is negligible compared to the unquenched rhodamine compound.[37]

As shown in Figure 10 NP-10 can be switched up to 22 times without a significant loss of the emission intensity. After approximately 23 switching cycles NP-10 slowly looses emission intensity, though the quenching efficiency stays the same. No change in the switching efficiency could be observed indicating that only the fluorophore undergoes photodegeneration rather than the photoswitch being destroyed in the process.

The calculated Förster radius for the rhodamine B–spiropyran system is $D_{eff}=6.16$ nm. From this data we calculated the experimental energy transfer efficiency of $E=89.5\,\%$ and the estimated average rhodamine B–spiropyran distance with 2.93 nm.

Although the samples prepared according to conditions B show smaller NP-sizes the switching properties are only slightly inferior to the ones obtained by conditions A. After several weeks the NP sedimented in ethanol/water suspension, but they could be resuspended by sonication. Considerable bleeding effects could not be observed because we only found traces of SP and RH in the solvent by NMR analysis.

Conclusion

We successfully prepared a range of nanoparticles covalently doped with a fluorophore and a photoswitch via Stöber condensation from TEOS and the precursors **1** and **2**. We observed a dependence of the NP size distribution by changing the concentration of fluorescence dye and photoswitch, consistent with the LaMer model for classical heterogeneous NP nucleation. Furthermore we succeeded in a constant form and size distribution even with high amounts of photoswitch and fluorophore and a size suitable for confocal and high resolution fluorescence microscopy. These NPs are capable of reversible fluorescence photoswitching by irradiation with UV/Vis light. Up to 22 cycles without any significant loss of fluorescence intensity were possible. The efficiency of switching differed depending on the molar ratios of photoswitch and fluorophore, but independent on size. The doped NPs did not show significant bleeding effects and other kind of decomposition, even after several weeks. In summary, we succeeded in the synthesis of tailor-made silica

based and switchable fluorescent nanoparticles with a high potential for bio-application. Future studies are in progress and are focused on clarifying the mechanism of fluorescence quenching and on improving its efficiency by selecting suitable pairs of donor and acceptors (in the sense of FRET) as well as developing silica nanoparticles of well-defined architectures aiming at applications in optical fluorescence microscopy.

Experimental Section

NMR spectra were measured at room temperature on a Bruker DRX 500 spectrometer (500 MHz). [D_4]Methanol was used as an internal standard for ^{1}H spectra. All UV/Vis absorption spectra were recorded in ethanol/water (1:1) on a Perkin–Elmer Lambda 25 UV/Vis spectrometer at room temperature. Fluorescence spectra were measured on a Perkin–Elmer 50 B fluorescence spectrometer.

For light-induced generation of the open form of the spiropyran the samples were irradiated at 365 nm using a Nichia diode. Fluorescence excitation of the fluorophores and photoswitching of the open to the closed form was induced by irradiation with 568 nm using a laser diode (Cube, Coherent). The resulting particle-solution was characterized by TEM (transmission electron microscopy - TWIN Philips CM 200). The sample preparation was carried out by dropping the particle solution on a carbon-coated TEM grid and removing the solvent under vacuum.

Synthesis of 3′,3′-dimethyl-1′-(β-hydroxyethyl)-6-nitrospiro[2*H*-1]benzopyran-2,2′-indoline (6): The experimental procedure followed for the synthesis of **6** starting from **3**, is the one reported by Raymo et al.[30]

Synthesis of 1′-(3-triethoxysilanpropyl)-3′,3′-dimethylnitrospiro[2*H*-1]benzopyran-2,2′-indoline (1): The experimental procedure followed for the synthesis of **1**, is the one reported by Allouche and Gonbeau.[29]

Synthesis of rhodamine B 4-(3-hydroxypropyl)piperazine amide (10): The experimental procedure followed for the synthesis of **10** starting from **8**, is the one reported by Nguyen and Francis.[31]

Synthesis of rhodamine B 4-(3-triethoxysilanpropyl)piperazine amide (2): A solution of rhodamine B 4-(3-hydroxypropyl)piperazine amide (**10**; 0.055 g, 0.096 mmol) and 3-triethoxysilylpropylisocyanate (**7**; 0.024 mL, 0.01 mmol) in dry DMF (20 mL) was stirred under reflux for 24 h. The emulsion of **2** was used without further purification. ^{1}H NMR (500 MHz, [D_4]MeOH): δ = 0.58(t, ^3J = 7, 4 Hz, 2H), 1.15 (t, ^3J = 7.2 Hz, 12H), 1.19 (t, ^3J = 7.1 Hz, 9H), 1.61 (m, 4H), 2.46 (t, ^3J = 7.2 Hz, 2H), 3.14 (t, ^3J = 7.2 Hz, 2H), 3.35 (br m, 8H), 3.47 (q, ^3J = 6.9 Hz, 6H), 3.67 (q, ^3J = 7.1 Hz, 8H), 4.12 (t, ^3J = 7.2 Hz, 2H), 6.93 (s, 1H), 6.96 (s, 1H), 7.05(d, ^3J = 9.5 Hz, 1H), 7.07 (d, ^3J = 9.6 Hz, 1H), 7.9 (d, ^3J = 9.6 Hz, 1H), 7.26 (d, ^3J = 9.5 Hz, 2H), 7.50 (m, 1H), 7.72 (m, 1H), 7.76 (m, 2H); ESI-MS (positive): m/z: 816.5 $[M]^+$.

Preparation of nanoparticles: The silica nanoparticles doped with the fluorophor (**2**) and the photoswitch (**1**) were prepared using a modified Stöber method.[29]

A mixture of ethanol, deionized water, and concentrated ammonia solution ≥25% (Roth) was stirred for 2 min. To this mixture, TEOS (Aldrich) was slowly added, after 5 min the fluorophor (**2**) and the photoswitch (**1**) were slowly added and the mixture was stirred at room temperature overnight. Two different molar ratios of TEOS/NH_3/EtOH/H_2O were used. A: TEOS (2 mL), ammonia solution (2 mL), double distilled water (6 mL), EtOH (100 mL). B: TEOS (4 mL), ammonia solution (4 mL), double distilled water (12 mL), EtOH (200 mL). The different molar ratios for **1** and **2** are given in Table 1, with concentrations of 0.09 M for **1** and 0.0031 M for **2**. For workup the reaction solutions were centrifuged with 3600 R/min over 15 min. After removing of the solvents the NP were dispersed in distilled water/ethanol (1:1; 50 mL). This process was repeated three times. To control the workup and analyze the different reaction setups TEM spectroscopy was used.

Acknowledgements

Support from the Deutsche Forschungsgemeinschaft (SFB 613) and from Bielefeld University is gratefully acknowledged.

[1] E. Abbe in *Archiv für Mikroskopische Anatomie, Band 9* (Ed.: M. Schultze), Springer, Berlin, **1873**, pp. 413–480; http://biodiversitylibrary.org/item/47676#page/423/mode/1up.
[2] B. Harke, J. Keller, C. K. Ullal, V. Westphal, A. Schönle, S. W. Hell, *Opt. Express* **2008**, *16*, 4154–4162.
[3] S. W. Hell, K. I. Willig, V. Westphal, *Biospektrum* **2006**, *12*, 492–494.
[4] M. Heilemann, S. van de Linde, M. Schüttpelz, R. Kasper, B. Seefeldt, A. Mukherjee, P. Tinnefeld, M. Sauer, *Angew. Chem.* **2008**, *120*, 6266–6271; *Angew. Chem. Int. Ed.* **2008**, *47*, 6172–6176.
[5] S. van de Linde, S. Wolter, M. Heilemann, M. Sauer, *J. Biotechnol.* **2010**, *149*, 260–266.
[6] H. Dürr, H. Bouas-Laurent, in *Photochromism, Molecules and Systems*, Elsevier, Amsterdam, **1990**, pp. 855–878.
[7] B. Feringa, in *Molecular Switches*, Wiley-VCH, Weinheim, **2000**, p. 399 ff.
[8] B. Seefeldt, R. Kasper, M. Beining, J. Mattay, J. Arden-Jacob, N. Kemnitzer, K. H. Drexhage, M. Heilemann, M. Sauer, *Photochem. Photobiol. Sci.* **2010**, *9*, 213–221.
[9] T. Förster, *Ann. Phys.* **1948**, *437*, 55–75.
[10] D. L. Andrews, D. S. Bradshaw, *Eur. J. Phys.* **2004**, *25*, 845–858.
[11] L. Giordano, T. M. Jovin, M. Irie, E. A. Jares-Erijman, *J. Am. Chem. Soc.* **2002**, *124*, 7481–7489.
[12] T. B. Norsten, N. R. Branda, *J. Am. Chem. Soc.* **2001**, *123*, 1784–1785.
[13] L. Zhu, M.-Q. Zhu, J. K. Hurst, A. D. Q. Li, *J. Am. Chem. Soc.* **2005**, *127*, 8968–8970.
[14] T. Stafforst, D. Hilvert, *Chem. Commun.* **2009**, 287–288.
[15] S. Bonacchi, D. Genovese, R. Juris, M. Montalti, L. Prodi, E. Rampazzo, N. Zaccheroni, *Angew. Chem.* **2011**, *123*, 4142–4152; *Angew. Chem. Int. Ed.* **2011**, *50*, 4056–4066.
[16] a) M. Montalti, L. Prodi, N. Zaccheroni, A. Zattoni, P. Reschiglian, G. Falini, *Langmuir* **2004**, *20*, 2989–2991; b) E. Rampazzo, S. Bonacchi, R. Juris, M. Montalti, D. Genovese, N. Zaccheroni, L. Prodi, D. C. Rambaldi, A. Zattoni, P. Reschiglian, *J. Phys. Chem. B* **2010**, *114*, 14605–14613.
[17] A. Burns, H. Ow, U. Wiesner, *Chem. Soc. Rev.* **2006**, *35*, 1028–1042.
[18] R. M. Yates, A. Hermetter, D. G. Russell, *Traffic* **2005**, *6*, 413–420.
[19] J. Fölling, S. Polyakova, V. Belov, A. van Blaaderen, M. L. Bossi, S. W. Hell, *Small* **2008**, *4*, 134–142.
[20] J. Chen, P. Zhang, G. Fang, P. Yi, X. Yu, X. Li, F. Zeng, S. Wu, *J. Phys. Chem. B* **2011**, *115*, 3354–3362.
[21] J. Chen, F. Zeng, S. Wu, J. Su, Z. Tong, *Small* **2009**, *5*, 970–978.
[22] J. Chen, F. Zeng, S. Wu, J. Zhao, Q. Chen, Z. Tong, *Chem. Commun.* **2008**, 5580–5582.
[23] L. Zhu, W. Wu, M.-Q. Zhu, J. J. Han, J. K. Hurst, A. D. Q. Li, *J. Am. Chem. Soc.* **2007**, *129*, 3524–3526.
[24] L. Wang, W. Tan, *Nano Lett.* **2006**, *6*, 84–88.
[25] T. K. Jain, I. Roy, T. K. De, A. Maitra, *J. Am. Chem. Soc.* **1998**, *120*, 11092–11095.
[26] J. Piard, R. Métivier, M. Giraud, A. Léaustic, P. Yu, K. Nakatani, *New J. Chem.* **2009**, *33*, 1420–1427.
[27] D. Genovese, M. Montalti, L. Prodi, E. Rampazzo, N. Zaccheroni, K. Altenhöner, F. May, J. Mattay, *Chem. Commun.* **2011**, *47*, 10975–10977.
[28] K. Kinashi, S. Nakamura, Y. Ono, K. Ishida, Y. Ueda, *J. Photochem. Photobiol. A* **2010**, *213*, 136–140.
[29] J. Allouche, A. Le Beulze, J.-C. Dupin, J.-B. Ledeuil, S. Blanc, D. Gonbeau, *J. Mater. Chem.* **2010**, *20*, 9370–9378.
[30] F. M. Raymo, S. Giordani, A. J. P. White, D. J. Williams, *J. Org. Chem.* **2003**, *68*, 4158–4169.
[31] T. Nguyen, B. M. Francis, *Org. Lett.* **2003**, *5*, 3245–3248.
[32] A. M. Powe, S. Das, M. Lowry, B. El-Zahab, S. O. Fakayode, M. L. Geng, G. A. Baker, L. Wang, M. E. McCarroll, G. Patonay, M. Li,

M. Aljarrah, S. Neal, I. M. Warner, *Anal. Chem.* **2010**, *82*, 4865–4894.
[33] S. W. Hell, *Science* **2007**, *316*, 1153–1158.
[34] V. K. LaMer, R. H. Dinegar, *J. Am. Chem. Soc.* **1950**, *72*, 4847–4854.
[35] V. Minkin, *Chem. Rev.* **2004**, *104*, 2751–2776.
[36] N. Shao, J. Jin, H. Wang, J. Zheng, R. Yang, W. Chan, Z. Abliz, *J. Am. Chem. Soc.* **2010**, *132*, 725–736.
[37] S. Zhang, Q. Zhang, B. Ye, X. Li, X. Zhang, Y. Deng, *J. Phys. Chem. B* **2009**, *113*, 6012–6019.
[38] J. L. Bahr, G. Kodis, L. de La Garza, S. Lin, A. L. Moore, T. A. Moore, D. Gust, *J. Am. Chem. Soc.* **2001**, *123*, 7124–7133.
[39] T. Minami, N. Tamai, T. Yamazaki, I. Yamazaki, *J. Phys. Chem.* **1991**, *95*, 3988–3993.

Received: September 21, 2011
Revised: November 13, 2011
Published online: December 28, 2011

